

1
2
3
4
5
6
7
8
9
10
11
12
13
14
15
16
17
18
19
20
21
22

Supplementary Information for

Formation mechanisms of atmospheric nitrate and sulfate during the winter haze pollution periods in Beijing: gas-phase, heterogeneous and aqueous-phase chemistry

Pengfei Liu, Can Ye, Chaoyang Xue, Chenglong Zhang, Yujing Mu*, Xu Sun

This PDF file includes:

- M1. Sample analysis for WSIs, OC and EC.
- M2. Measurements for atmospheric H₂O₂ and HONO.
- M3. The Mass transport for multiphase reactions.
- Figure S1. The location of the sampling site.
- Figure S2. Time series of meteorological parameters (wind speed, wind direction, ambient temperature and RH), O₃ and PM_{2.5} during the sampling period.
- Figure S3. The correlations between the concentrations of PM_{2.5} and CO in the three cases during the sampling period.
- Figure S4. The average mass proportions of the species in PM_{2.5} in the three cases during the sampling period.

23 ***Supplementary Information:***

24 **M1. Sample analysis for WSIs, OC and EC**

25 As for the filter samples, half of each filter was extracted ultrasonically with 10 mL ultrapure
26 water for 30 minutes. The supernatants were filtered by a type of microporous membrane (diameter,
27 13mm; pore size, 0.45 μm) and the WSIs in the filtrates were analyzed by an ion chromatography
28 (Wayeal IC6200, China). Five cations (Na^+ , K^+ , Ca^{2+} , Mg^{2+} and NH_4^+) were separated through a
29 cation column (TSKgelSuperIC-CR, 4.6 mm ID \times 15 cm) with the solvent (2.2 mmol L^{-1} methane
30 sulfonic acid and 1 mmol L^{-1} 18-crown-6) flow rate of 0.7 mL min^{-1} and column temperature of 40
31 $^{\circ}\text{C}$. Four anions (Cl^- , NO_3^- , SO_4^{2-} and NO_2^-) were separated via an anion column (IC SI-52 4E, 4.0
32 mm ID \times 25 cm) with the solvent (3.6 mmol L^{-1} sodium carbonate) flow rate of 0.8 mL min^{-1} and
33 column temperature of 45 $^{\circ}\text{C}$. The relative standard deviation (RSD) of each ion was not more than
34 0.5 % for the reproducibility test. The detection limits ($S/N=3$) were less than 1 $\mu\text{g L}^{-1}$ for the cations
35 and anions. At least three filter blanks were simultaneously analyzed for every 60 filter samples,
36 and the mean blank values were about 30 $\mu\text{g L}^{-1}$ for Na^+ , Ca^{2+} , NO_2^- , NO_3^- and SO_4^{2-} , 20 $\mu\text{g L}^{-1}$ for
37 NH_4^+ and Cl^- , 10 $\mu\text{g L}^{-1}$ for Mg^{2+} and K^+ . All ion concentrations were corrected for the blanks.

38 A quarter of each filter was heated with temperature programming to 140 $^{\circ}\text{C}$, 280 $^{\circ}\text{C}$, 480 $^{\circ}\text{C}$
39 and 580 $^{\circ}\text{C}$ in the helium atmosphere for analyzing OC1, OC2, OC3 and OC4, respectively, and then
40 to 580 $^{\circ}\text{C}$, 780 $^{\circ}\text{C}$ and 840 $^{\circ}\text{C}$ in the atmosphere of 98 % helium and 2 % oxygen for analyzing EC1,
41 EC2 and EC3, respectively, by using a thermal optical carbon analyzer (DRI-2001A). The pyrolyzed
42 OC (POC) is defined as the carbon fraction that has combusted after the initial introduction of
43 oxygen and before the laser reflectance signal returns its original value, and it is assigned to the OC
44 fraction (Ma et al., 2016;Zhang et al., 2013). Then, $\text{OC} = \text{OC1} + \text{OC2} + \text{OC3} + \text{OC4} + \text{POC}$ and EC

45 = EC1 + EC2 + EC3 – POC. The method calibration was performed with a concentration gradient
46 of KHP standards ($R^2 = 0.9997$, $N=5$). A replicate sample was detected for every 10 filter samples,
47 and the RSD of OC and EC was less than 5 %. The detection limits were $0.82 \mu\text{gC cm}^{-2}$ and 0.20
48 $\mu\text{gC cm}^{-2}$ for OC and EC, respectively.

49 **M2. Measurements for atmospheric H₂O₂ and HONO**

50 Atmospheric H₂O₂ was measured by a wet liquid chemistry fluorescence detector (AL 2021;
51 AERO laser, Germany). When atmospheric H₂O₂ is stripped by a faintly acid solution (pH = 5.8-
52 6.0), organic peroxides are simultaneously detected by the catalysis of the horseradish peroxidase
53 and then the reaction with *p*-hydroxyphenyl-acetic acid. In order to divide between H₂O₂ and organic
54 peroxides, two channels are designed and H₂O₂ is selectively destroyed by catalase prior to the
55 detection of fluorescence in one channel. Thus, the difference of the signal between the two channels
56 can represent the H₂O₂ concentration. The calibrations were performed with liquid H₂O₂ standards
57 ($33.3 \mu\text{g L}^{-1}$) for both channels in every 1-3 days. There is an uncertainty of 10 %, a calibration RSD
58 of 0.25 %, a detection limit of less than 50 ppt and a noise of less than 2 % at full scale for the H₂O₂
59 monitor. Although some organic peroxides such as HOCH₂OOH and CH₃C(O)OOH have been
60 found to decompose into H₂O₂ in the collection solution at pH > 5 (O'Sullivan, 1996), their
61 decomposition to H₂O₂ during the short period of the sampling progress could be neglected due to
62 their relatively slow hydrolysis rate (1–2 days) (O'Sullivan, 1996) and extremely low atmospheric
63 concentrations (He et al., 2010).

64 Atmospheric HONO was measured by a wet chemical method that is named after stripping coil
65 (SC) equipped with ion chromatograph (IC) and was described in detail by our previous studies
66 (Xue et al., 2019a; Xue et al., 2019b). Briefly, hourly HONO samples were absorbed by ultrapure

67 water in the SC with the gas flow rate of 2 L min⁻¹ and the absorption solution flow rate of 0.2 mL
 68 min⁻¹. After sampling, the liquid samples were stored in a refrigerator around 4 °C and then analyzed
 69 by IC in three or four days. The flow calibrations including the gas and liquid were performed once
 70 a day, and the collection efficiency was more than 90 % and the correlations between the SC-IC and
 71 other techniques were close to 0.9 (slope = 0.94~1.06) (Xue et al., 2019a).

72 M3. The Mass transport for multiphase reactions

73 The formula of a standard resistance model was adopted for evaluating the effects of mass
 74 transport (Seinfeld and Pandis, 2006):

$$75 \quad \frac{1}{R_{S, aq}} = \frac{1}{R_{aq}} + \frac{1}{L_{aq, lim}} \quad (\text{S-R1})$$

76 where $R_{S, aq}$ is the sulfate production rate, R_{aq} is the aqueous-phase reaction rate of oxidants
 77 which could be calculated by the equations of R1-R4, and $L_{aq, lim}$ is the limiting mass transfer rate
 78 (M s^{-1}) which could be calculated by the formulas as follows (Seinfeld and Pandis, 2006):

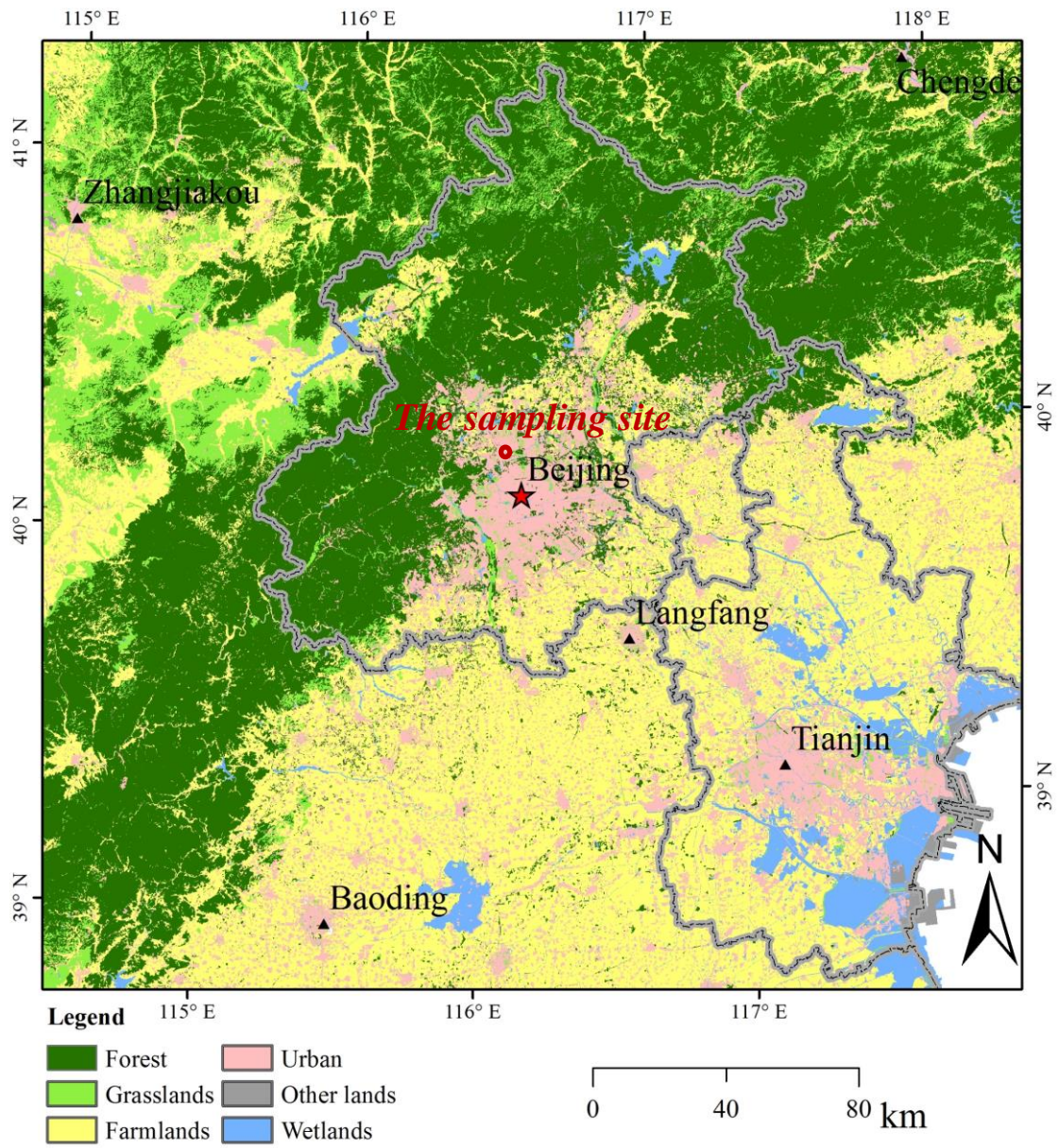
$$79 \quad L_{aq, lim} = \min\{L_{aq}(SO_2), L_{aq}(O_{xi})\} \quad (\text{S-R2})$$

$$80 \quad L_{aq}(X) = k_{MT}(X) \cdot [X] \quad (\text{S-R3})$$

81 where $[X]$ represents the aqueous-phase concentrations of SO_2 or the oxidants O_{xi} such as O_3 ,
 82 H_2O_2 and NO_2 , which could be calculated based on Henry's law (R5-R7). The mass transfer rate
 83 coefficient $k_{MT}(X)$ (s^{-1}) is expressed by the equations as follows (Seinfeld and Pandis, 2006):

$$84 \quad k_{MT}(X) = \left[\frac{R^2}{3D} + \frac{4R}{3\alpha v} \right]^{-1} \quad (\text{S-R4})$$

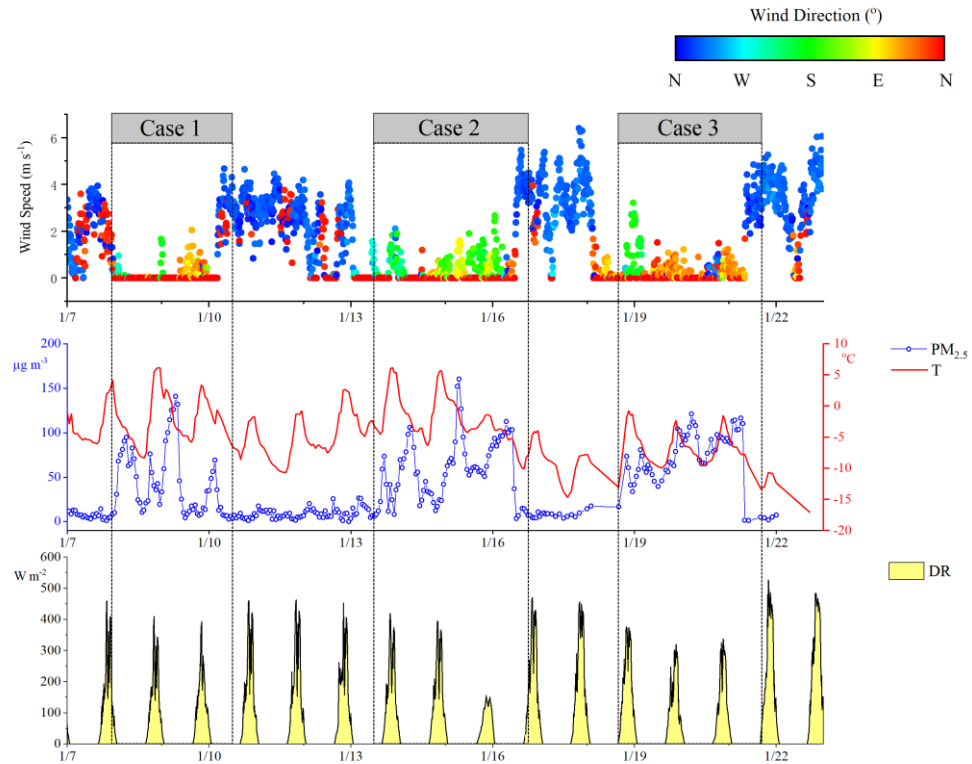
85 where R is the aerosol radius (0.15 μm), D is the gas-phase molecular diffusion coefficient (0.2
 86 $\text{cm}^2 \text{s}^{-1}$ at 293 K), v is the average molecular speed ($3 \times 10^4 \text{ cm s}^{-1}$), and α is the mass accommodation
 87 coefficient (0.11, 0.23, 2×10^{-3} and 2×10^{-4} for SO_2 , H_2O_2 , O_3 and NO_2 , respectively) on the droplet
 88 surface (Jacob, 2000; Seinfeld and Pandis, 2006).



90

91

Figure S1. The location of the sampling site.

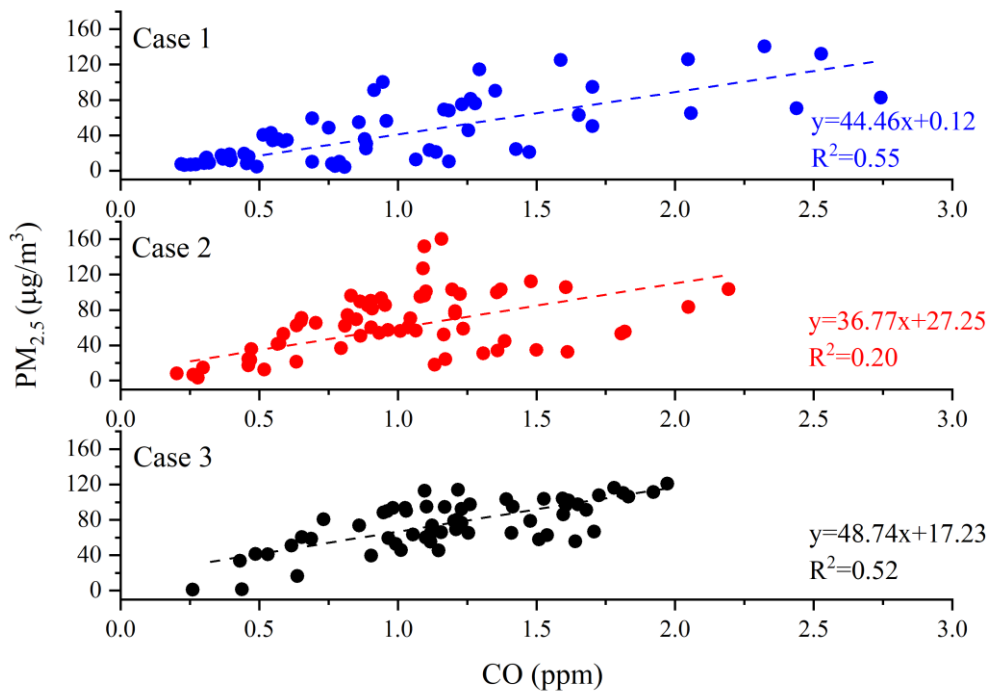


92

93

Figure S2. Time series of meteorological parameters (wind speed, wind direction, ambient temperature and DR) and PM_{2.5} during the sampling period.

94



95

96

Figure S3. The correlations between the concentrations of PM_{2.5} and CO in the three cases during the sampling period.

97

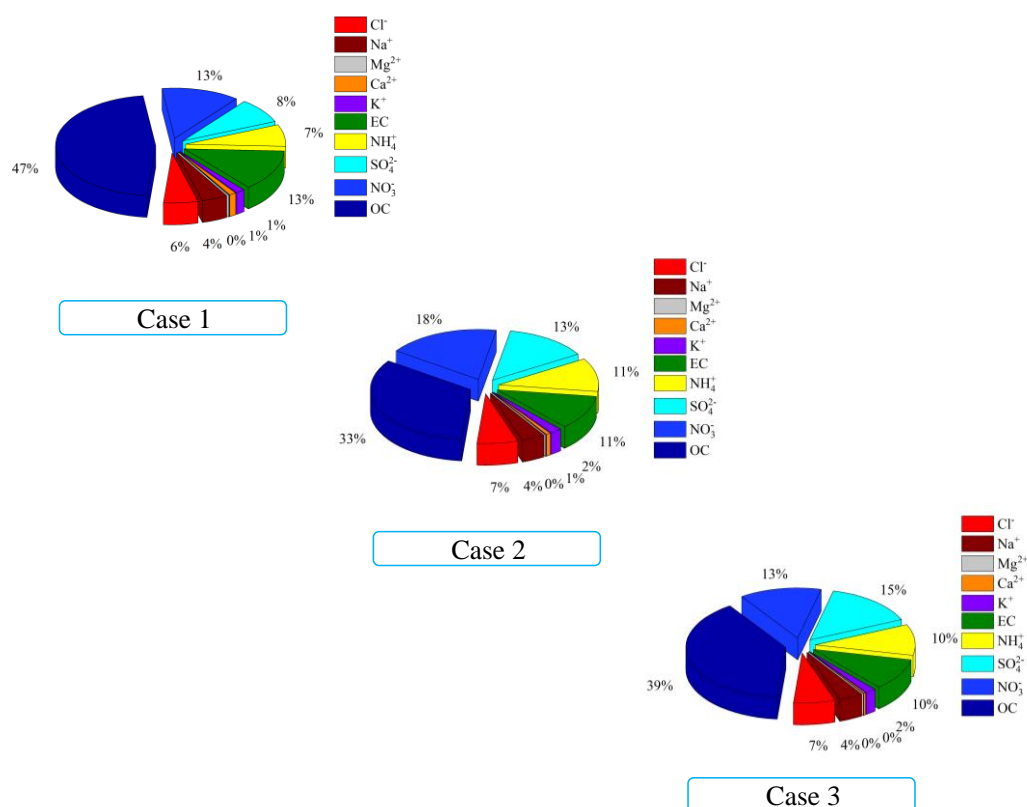


Figure S4. The average mass proportions of the species in PM_{2.5} in the three cases during the sampling period.

References

He, S. Z., Chen, Z. M., Zhang, X., Zhao, Y., Huang, D. M., Zhao, J. N., Zhu, T., Hu, M., and Zeng, L. M.: Measurement of atmospheric hydrogen peroxide and organic peroxides in Beijing before and during the 2008 Olympic Games: Chemical and physical factors influencing their concentrations, *Journal of Geophysical Research*, 115, 10.1029/2009jd013544, 2010.

Jacob, D. J.: Heterogeneous chemistry and tropospheric ozone, *Atmospheric Environment*, 34, 2131-2159, 2000.

Ma, X., Wu, J., Zhang, Y., Bi, X., Sun, Y., and Feng, Y.: Size-Classified Variations in Carbonaceous Aerosols from Real Coal-Fired Boilers, *Energy & Fuels*, 30, 39-46, 10.1021/acs.energyfuels.5b01770, 2016.

O'Sullivan, D. W. J. J. o. P. C.: Henry's Law Constant Determinations for Hydrogen Peroxide, Methyl Hydroperoxide, Hydroxymethyl Hydroperoxide, Ethyl Hydroperoxide, and Peroxyacetic Acid, 100, 3241-3247, 1996.

Seinfeld, J. H., and Pandis, S. N.: *Atmospheric Chemistry and Physics, from Air Pollution to Climate Change*, Wiley, 429-443 pp., 2006.

Xue, C., Ye, C., Ma, Z., Liu, P., Zhang, Y., Zhang, C., Tang, K., Zhang, W., Zhao, X., Wang, Y., Song, M., Liu, J., Duan, J., Qin, M., Tong, S., Ge, M., and Mu, Y.: Development of stripping coil-ion chromatograph method and intercomparison with CEAS and LOPAP to measure atmospheric HONO, *The Science of the total environment*, 646, 187-195, 10.1016/j.scitotenv.2018.07.244, 2019a.

122 Xue, C., Ye, C., Zhang, Y., Ma, Z., Liu, P., Zhang, C., Zhao, X., Liu, J., and Mu, Y.: Development
123 and application of a twin open-top chambers method to measure soil HONO emission in the North
124 China Plain, *Sci. Total Environ.*, 659, 621-631, 10.1016/j.scitotenv.2018.12.245, 2019b.
125 Zhang, R., Jing, J., Tao, J., Hsu, S. C., Wang, G., Cao, J., Lee, C. S. L., Zhu, L., Chen, Z., Zhao, Y.,
126 and Shen, Z.: Chemical characterization and source apportionment of PM_{2.5} in Beijing: seasonal
127 perspective, *Atmospheric Chemistry and Physics*, 13, 7053-7074, 10.5194/acp-13-7053-2013, 2013.